SINET: Ethiop. J. Sci., 47(1): 1-16, 2024 ISSN: 0379–2897 (PRINT)
 eISSN: 2520–7997

Date received: -October 2023-; Date revised: -June 2024-; Date accepted: -August 2024
DOI: https://dx.doi.org/10.4314/sinet.v47i1.1

Prediction of the effect of climate covariates on wind potential in Ethiopia

Bedanie Gemechu Bulty[1]*, Butte Gotu[2] Gemechis Djira[3], Joep Crompvoets[4]

[1]*Department of Statistics, Ambo University, Ambo, Ethiopia
[2]Department of Statistics, Addis Ababa University, Addis Ababa, Ethiopia
[3]Department of Mathematical Statistics, State University of South Dakota, USA
[4]Department of Geospatial Sciences, at KU Leuven, Belgium

ABSTRACT: This study explores the interaction of climate covariates and spatial elements with wind speed in Ethiopia. It intends to extrapolate the potential spots of wind at unobserved spatial points using a meteorological dataset. We applied a combined dynamic spatial panel autoregressive random effects model with a spatial weight of inverse quartile separation distances of locations. This spatial weight outperforms the other spatial weights to capture spatial dependence and gain efficient estimates. The result describes that mean wind speed varies over the longitude range and latitude span, is influenced by climate covariates and fluctuates over the months of a year. Wind speed intensity is high along the central, eastern and northeastern parts of the region. It is also high in February, March, June, and July relative to September and October months. The evidence shows that wind speed is higher in summer and spring but relatively lower in winter and fall seasons. This implies that wind speed is high mainly after the rainy season ends and before it starts. The model estimates also show that mean wind speed is spatially correlated across neighboring stations and over temporal points. Particularly, the mean wind speed increases with altitude and temperature but decreases as precipitation increases. Sunshine fraction and relative humidity have negative effects, but their influence is not statistically significant with p=0.2496 and p=0.4484 respectively. In conclusion, the methods are recommended for the prediction of data that exhibits a stochastic process.

Keywords: Bayesian inferences; Dynamic spatial panel autoregressive model, Prediction, spatial weights of inverse quartile separation distances, Stochastic process

INTRODUCTION

Climate change threats and the stochastic nature of wind energy sources have become major global issues (Yao et al., 2012). Every society requires energy supply to meet basic human needs (e.g., lighting, cooking, space comfort, mobility, communication) and to serve productive processes. For sustainable development, delivery of energy services needs to be secure with low environmental impacts. Therefore, the efforts of many countries to build green energy have started with the introduction of renewable energy systems in their future energy plans and policies. However, energy supply distribution from renewable resources is uneven and had been dominated by few countries such as China, the United States and the United kingdom (Yamba et al., 2011; Belward et al., 2011).

One of the most abundant renewable energy resources is wind, although Africa's share is very low regardless of its potential (Olabi, 2013). The production of wind energy is influenced by various local climatic and spatial variables, and its distribution varies over time (Yao et al., 2012). All renewable energy resources including wind are highly susceptible to local variations in climate making their predictions challenging. Thus, for effective production of wind energy, the

*Author to whom correspondence should be addressed.

first measure that has to be taken is conducting an adequate survey of wind availability. However, the fluctuation of the mean wind speed makes it difficult to obtain reliable estimates of wind availability. Consequently, wind models have been developed based on available mean wind speed data records (Kadhem, 2017).

Ethiopia is at the forefront in terms of its wind potential in Africa. According to a report on wind energy conditions in Ethiopia, there is approximately 1350 GW (>7 m/s) exploitable reserve of wind energy, of which only less than 1% has been developed (Derbew, 2013). However, the site selection of potential spots is highly subjected to climatic variability (global and local) and spatial factors, which directly affect the production of wind power. A potential spot census has not been completed for the vast overland wind resource-enriching regions using reliable scientific methods in Ethiopia. Wind speed potential assessment in Ethiopia was carried out in hybrid system for off-grid rural electrification by Bekele and Tadesse (2012) and the annual average wind speed at a nearby station (Debre Markos), the study area, was calculated as 3.5 m/s based on anemometer data collected at 10m height. The minimum of the 3.5 m/s and the 3.1 m/s, measured on the data obtained from NASA evidenced to the belief that unevenness nature of the upper Blue Nile gorge is a good resource of wind, the northern part of Ethiopia. However, this area is high-relief area and is difficult to utilize the wind resources. A stand wind power supply system was considered for four locations; Addis Ababa, Mekele, Nazret and Debrezeyt (Bekele and Palm, 2010). The monthly average wind speeds for the locations showed relative increase from January to April and September to November but mild in the months of June to August.

Many previous studies across developed countries have relied on climate models that require a high-resolution downscaling approach. However, the statistical downscaling technique is deficient in determining all uncertainties at increased spatial resolution (Gonz´alez Aparicio et al., 2017). Prediction of wind power or climate variates has often been carried out using the General Circulation Model (GCM) or the Regional Climate Model (RCM) (Yao et al., 2012). Breslow and Sailor (2002) conducted a study on the vulnerability of wind power resources to climate change in the continental United States using GCM output from the Canadian Climate Center and Hadley Center to provide a range of possible variations in seasonal mean wind magnitude. The projection predicted that wind speed will reduce from 1.0 to 3.2% in 50 years, and 1.4 to 4.5% over 100 years. Another downscaling approach involves RCMs that run over a limited spatial domain. However, no spatial dependence measure was considered and the prediction was also limited to small spatial scales from 100 to 200 km (Greasby, 2011). The reanalysis method has been frequently used for the quantification of mean wind speed, and wind power in many studies. However, it does not have a time variation property, and excludes cross-dependence between meteorological data which may not be able to capture local wind features (Kadhem et al., 2017). Wind potential spot can be estimated based on various local environmental factors and global factors using common geostatistical models. As climate variables vary across space and time, we seek to identify areas across the domain (or regions) that might influence wind distribution. Dominantly, temperature measures have been used as a predictor to model wind distribution in previous studies, where many other climate and spatial variables could have significant effects. Thus, geostatistical models do not capture the stochastic nature of wind and climate variables by customary spatial dependence measures.

In most empirical studies, it is difficult to measure uncertainty in the spacetime stochastic processes. For instance, the stochastic nature of the power production system arises from uncertainty in spatial resolution particularly for wind power. The

measurement of spatial and time effects is not easy, as in the case of pure time series and when the data structure is flipped from the customary cross-sections to the spatial panel setting. Difficulties in determining the effects of spatial autocorrelation or spatial heterogeneity are commonly interrelated, causing model identification and misspecification problems (Harris et al., 2003; cited in Elhorst, 2011). In addition, involving all possible spatial interaction effects causes problems in parameter identification and overfitting. In such cases, we prefer to choose among simpler models with less spatial interaction effects (Elhorst, 2011).

Due to expensive installation costs of wind energy, it requires a careful planning and assessment of wind potential spots. Once a potential spot is identified, a proper siting of the wind turbine and location greatly determines the wind resource management. Wind measurement and mapping should also be carried out over a long period (at least one year) to integrate the different seasonal variations prior to installation. However, the availability of data is the big challenge for the sustainable wind power harvest.

Therefore, this study lays a foundation towards understanding the trends of wind distribution, the effects of climate covariates and topographic elements on mean wind speed which varies over space and time. It uses a combined dynamic spatial panel autoregressive model with spatial weight based on inverse quartile separation distances to analyze the effects of climate covariates on wind distribution.

In this paper, we also considered the spatial plots and dynamic spatial panel autoregressive model with an alternative spatial weight design (Bulty et al., 2023). As such, Bayesian hierarchical modelling is also used for prediction (or estimation) over traditional likelihood-based methods to gain the more efficiency in the estimates. The performance attained through the use of the spatial weight matrix of inverse quartile separation distances of locations is better as compared with the state of the art of the works. Explicitly, the contiguity-based spatial weight is not the best option for stochastic processes distributed over large spatial regions since it disregards higher level neighborhood relationships, when two locations may be indefinitely neighbors to each other with decreasing magnitude as the locations get far apart. Euclidean distance based spatial weight is not also an appropriate measure of adjacency for spatial variables since it considers a straight-line distance in two dimensional space and is influenced by the accuracy of the distance measures. The data for this study was obtained from records of continuous measurement carried out by National meteorological Agency of Ethiopia from 2000 to 2017 at 60 stations. Obviously, wind power is mathematically related to wind speed in cubic scale, and thus the prediction of mean wind speed leads to the prediction of wind power.

Following the last paragraph in Sec.1, Sec. 2 describes the methods of prediction, Sec. 3 is about the presentation and discussion of the results of the study, and Sec 4 concludes the result of the study and recommends for the best spot of wind.

METHODOLOGY

This section discus about the statistics, natural condition and wind potential area assessment in the study region. It also describes the scientific methods employed for the prediction of wind potential spots and its interaction with climate and spatial variables.

Description of Wind Potential Spatial Domain

The Federal Democratic Republic of Ethiopia (FDRE) is the most populous, landlocked, fast-growing non-oil-producing country in the Horn of Africa. The total area of

the country is approximately 1.104 million square kilometers with a population of approximately 107 million according to the latest United Nations projection in 2018. Of the total population, 83% live in rural areas with limited or no access to electricity.

Ethiopia has four seasons namely; summer (*kiremt*)- June to August, spring (*tsedey*)- September to November, winter (*bega*)- December to February and fall (*belg*)- March to May. However, latitudes and topographic conditions vary from place to place; therefore, the transition time of the seasons differs from region to region within the country. Summer (kiremt), the rainy season is characterized by abundant rainfall which is an essential condition for the production and life of local people as well as a basis for local irrigation farming. Drought during this season may be disastrous for people in the entire Nile Basin, including Ethiopia (Jiangtao, et al., 2012).

Hydrochina Corporation prepared the first wind and solar energy master plan for Ethiopia in 2012. The report focused on the assessment of wind and solar energy resources based on meteorological data, observations of wind masts, and numerical simulation methods (Jiangtao et al., 2012). It is believed that the complex topographic conditions of Ethiopia are important causes for the formation of wind energy resources. Because of regional differences in latitude, elevation, topographic conditions, Earth surface conditions, and other external conditions, wind energy resources have complicated and diversified compositions and distribution in different regions of Ethiopia. The distribution of wind energy resources has four major regions: the Great Rift Valley, mid-north highland, west low-relief, and east Somali plain regions.

The basic north-east to south-west strike of the East African Great Rift Valley in Ethiopia approaches the northeast trade winds. Moreover, under the venturi effect of the Great Rift Valley and the forced acceleration action of mega relief, vast regions rich in wind energy resources form in the Rift zone and on both sides. Consequently, these regions have become major target regions for wind power development in Ethiopia, according to the master plan.

The mid-north highland region of Ethiopia mainly includes the middle of Oromia State, most of Amhara State and the mid-east of Tigray State. This region is the principal part of the Ethiopian highlands. In this region, plateau tablelands and mountainous lands are widely distributed and many zones rich in wind energy resources are usually in high-relief areas. However, it is difficult to develop and utilize these resources because of their complex terrain. The western part of Ethiopia is mainly a large area near the boundaries of Sudan and South Sudan. With the gradual fall of relief in the region, the forced acceleration action of the terrain weakens, and the wind speed on the surface layer is low; thus, wind energy resources are limited. The Ethiopian east plain region mainly refers to a large area of the Somali region, which is broad and has small relief. All year round, the region has strong winds under the alternative influence of the northeast trade wind zone and southwest monsoon zone. Moreover, the regions rich in wind energy resources are centralized along the Great Rift Valley, from the capital Addis Ababa to Mekele in the north and from Addis Ababa to Mega in the south (Ethiopian Wind Energy Agency, 2009). It also includes the east and the west sides of the Great Rift Valley, from the capital city to eastwards up to Harar and Jijiga towns. Therefore, this study is limited to the potential areas described in Figure 1.

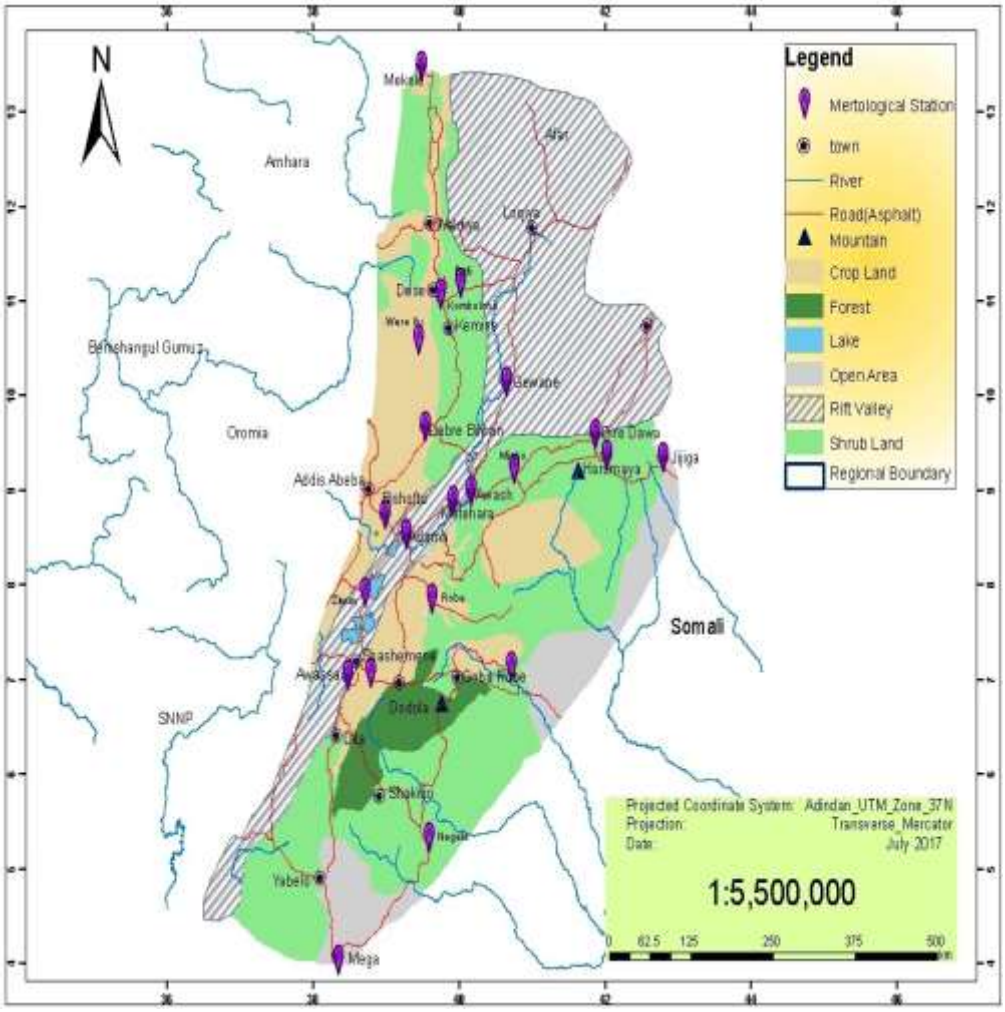

Figure 1: Wind Potential Areas of Ethiopia- The Study Area (primary; 2017)

Data Sources

The units used in the analysis are meteorological elements that are point-referenced spatially continuous processes and temporally discrete data, which is obtained from records of National Meteorological Agency of Ethiopia for the period January 2000 to December 2017 taken at 60 stations. The dataset includes monthly observed data of wind speed (m/s), temperature (maximum and minimum) in ^{0}C, relative humidity (%), rainfall or precipitation (mm), and sunshine fraction (h). In addition to meteorological elements, spatial elements such as elevation, longitude (easting) and latitude (northing) at each station were included. A spatial panel data frame ordered first in time and then in space is used for which each record reflects a single time and space combination.

Stations found in Ethiopian east plain region and along the Great Rift Valley zone are identified as the abundant potential regions for harvesting wind energy in Ethiopian according to the wind and solar energy assessment master plan. Consequently, an opportunistic design as indicated by Diggle et al. (2007) is considered, whereby continuous field data are taken from the selected stations in the region (R), which vary over the eastern plain of the country and towards the Great Rift Valley zones.

There are 37 surface-based Automatic Weather Stations (AWS) at various locations in Ethiopia. These stations report wind speed

and direction, temperature, relative humidity, radiation, and rainfall every 15 minutes. There are also special stations for air navigation at some airports called automatic weather observing system (AWOS). In addition, available wind masts in a few regions of the country were used, but they could not adequately provide valid information across the country. The stored data has coverage problem as the stations are located in large towns and data gaps due to interruptions of observations.

Method of Prediction

The existing stations in the study region are selected from over-dispersed large spatial scales where this study has no full control of every record at each station. There is dominantly a north-east trade wind that continuously flows from north to east. Thus, records at each station show higher similarity in orientation and hence, the orientation effects assumed to be negligible. Very often, during winter season, the weather is sunny and dry with strong radiation, bringing rich wind energy and solar energy. With the coming of summer in Northern Hemisphere, subtropical high pressure in North Africa moves northwards thus trade-wind zone also moves northwards. Besides, the study region is mostly a plain field and there are no or little wind barriers that affect the direction of wind from its natural flow. Also, the sitting of the stations with wind records are situated so as to avoid the effects of local topographic barriers. Even though the influence of wind direction is very essential to the subject, it is negligible and so, the use of anisotropic models takes on distinct model specifications. Therefore, the assumption of isotropic condition for stationarity in the space and time generally holds. From the three core spatial autoregressive models, the dynamic spatial panel autoregressive model containing both interaction effects among the error terms and endogenous interaction effect has more practical values when all locations are assumed to be neighbours to each other in the neighbourhood structure set up.

We have two techniques in spatial interpolations (or predictions), namely distance-based and geostatistics methods. When distance-based technique is chosen, we need to define a certain neighborhood that would be integrated into the model (Flitter et al, 2016). This paper employs a specific dense spatial weight design of inverse quartile of separation distances between stations pertaining to the recent works by Bulty et al. (2023). The separation distances between spatial locations is great-circle distances calculated using *haversine* formula. The *Haversine* formula is given by,

$$a = \sin^2(\frac{\Delta\theta}{2} + \cos\theta_1 \times \cos\theta_2 \times \sin^2(\frac{\Delta\delta}{2})) \quad (1)$$

$$C = 2a \times \tan 2(\sqrt{a}, \sqrt{(1-a)})$$

$$d = R \times C,$$

where θ_1 and θ_2 are the latitudes of the radius, $\Delta\theta$ is the latitude difference ($\Delta\theta=\theta_1-\theta_1$), $\Delta\delta$ is the longitude difference ($\Delta\delta=\delta_1-\delta_1$)) and R is radius of the earth (mean radius=6371km).

The measures of separation distances are grouped into intervals according to their positions relative to the quantile values and weighted to the inverse of their respective quairtile values. Briefly, let s_i and s_j be the ith and jth locations, respectively. Then, $d_{ij} = | s_i - s_j |$ is the absolute separation distance between locations i and j in kilometers, and Q_n denotes the nth quantile value. Furthermore, $l(d_{ij})$ denotes a function of separation distance between pairs of locations. The weights are computed for each level of neighbors using the inverse quartile of separation distances between locations. Thus, $l(d_{ij})$ can be defined as;

$$l(d_{ij}) = \begin{cases} \frac{1}{Q_1}, & 0 < d_{ij} \leq Q_1 \\ \frac{1}{Q_2}, & Q_1 < d_{ij} \leq Q_2 \\ \frac{1}{Q_3}, & Q_2 < d_{ij} \leq Q_3 \\ \frac{1}{U_0}, & Q_3 < d_{ij} \leq U_0 \end{cases} \quad (2)$$

There are N^2-N nonzero links in the matrix, where N is the number of diagonal elements of the weight matrix in each interval. Thus, the weights, w_k are assigned as,

$$w_{ij} = \begin{cases} l(d_{ij}), & 0 < d_{ij} \leq U_0 \\ 0, & d_{ij} = 0 \end{cases} . \quad (3)$$

The weights matrix, W_N is zero on-diagonal (i.e. $w_{ij} = 0$, for $i = j$, $i, j = 1,...,N$) and non-zero off-diagonals (w_{ij}, for $i \neq j$), where N is the number of locations and is given as,

$$W_N = \begin{bmatrix} 0 & \cdots & w_{1N} \\ \vdots & \ddots & \vdots \\ w_{N1} & \cdots & 0 \end{bmatrix} \quad (4)$$

The spatial weight matrix is normalized by making the entries in the rows to add up to one. That is, the weights are then, row-standardized (row sum is unity) to constitute the elements of the weight matrix.

$$\bar{W}_N = \frac{w_{ij}}{w_{i+}} , \quad (5)$$

Where $w_{i+} = \sum_j w_{ij}$ is the row-sum. Thus, the normalized weights matrix,

$$\widetilde{W}_N = \begin{bmatrix} 0 & \cdots & \widetilde{w}_{1N} \\ \vdots & \ddots & \vdots \\ \widetilde{w}_{N1} & \cdots & 0 \end{bmatrix} \quad (6)$$

It provides the spatial weight matrix, $\widetilde{W}_N$ of full rank and positive definite, and assumed to be constant over time (or static spatial weights). Using the subscripts to designate the matrix dimension, with $\widetilde{W}_N$ as the weight matrix for the cross-sectional or spatial dimension, and observations stacked or pooled in regression, the full $NT \times N$ weight matrix becomes,

$$\widetilde{W}_{NT} = I_T \otimes \widetilde{W}_N \quad (7)$$

I_T is the identity matrix of dimension $T \times 1$ for T temporal points, and $\widetilde{W}_N$ is a spatial weight matrix of dimension $N \times N$, where N is the number of locations and $\otimes$ is Kronecker product operator. The shift operator for the time component (e.g., time lag) is directly incorporated into the A combined dynamic spatial panel autoregressive model (Anselin et al., 2004). A combined dynamic spatial panel autoregressive model is specified as,

$$yt = \lambda(IT \otimes WN)yt + \varphi 1 yt-1 + \varphi 2(IT \otimes WN)yt-1 + X t\beta + a\mathbf{1}N + \mu + \psi t\mathbf{1}N + ut$$
$$u_t = \rho(I_T \otimes W_N)u_t + \varepsilon_t, \quad (8)$$

Where, y_t denotes an N×1 vector of dependent variable for every unit in the sample $i = 1,...,N$ at time t ($t = 1,...,T$), y_{t-1} denotes an N×1 vector of time-lagged dependent variable, φ_1 and φ_2 are scalar measures of strengths of time lag correlation and spacetime lag correlations, respectively. $(I_T \otimes W_N)y_{t-1}$ denotes a spacetime lag endogenous interaction effect component, $(I_T \otimes W_N)y_t$ denotes spatial lag endogenous interaction effect component associated with a spatial autoregressive coefficient λ, X_t denotes an N×K matrix of exogenous explanatory variables with the associated parameter β, $\mathbf{1}_N$ denotes an N×1 vector of ones associated with a constant a, μ is N×1 vector of spatial fixed or random effects, ψ_t is time period fixed effects. $(I_T \otimes W_N)u_t$ denotes spatial interaction effects among error terms and ε_t is an N×1 vector of disturbance terms (Bulty et al., 2023).

We used the maximum likelihood estimation (MLE) method for spatial panel dataset. Since the posterior distribution is proportional to the product of the data, process and parameter models, sampling can be accomplished using standard Markov Chain Monte Carlo (MCMC) techniques such as Gibbs sampler (Leeds and Wikle, 2012). The parameters are functions of the hyperparameters with their respective conditionally independent set or noninformative priors. In this paper, however, the default values (noninformative) of the priors in the *LearnBayes* package are applied to get appropriate Bayesian estimates (Albert, J., 2018).

RESULTS AND DISCUSSIONS

Spatial Panel Data Description

Meteorological dataset is described using simple tables and spatial plots. Primarily, 18 years dataset is aggregated into 12 months

across 60 stations to get a spatial panel data structure of 720 observations of spacetime stack. Such aggregation leads to a balanced panel data which simplifies computational difficulties in spatial panel data models.

The means of measurements have been simulated from 1000 samples based on the data at 95% confidence level. The results shown in Table 1 reveal that, the study region is found in the elevation range of 376 meter and 3084 meter with a credible set of mean to be from 1679.13 to 1779.37 meter. It is located in the longitude range of 36.20 ^{0}E to 44.30 ^{0}E and from 4.88 ˚N to
13.88 ˚N latitude span.

Table 1. Summary of Meteorological Dataset.

Variables	Mean	Min.	Max.	sd	95% Credible set for the means
Elevation (meters)	1729	376	3084	678.1	(1679.13, 1779.37)
Longitude(degree)	39.65	36.20	44.30	1.59	(39.54, 39.77)
Latitude (degree)	8.84	4.88	13.88	2.29	(8.69, 9.01)
Wind speed (m/s)	1.62	0.10	7.10	0.85	(1.56, 1.69)
Temperature (Max, ^{0}C)	27.63	13.53	43.13	5.54	(27.23, 28.04)
Rainfall, precipitation (mm)	67.66	0	381.40	68.62	(62.48, 72.37)
Relative Humidity (%)	62.39	36.75	90.80	9.79	(61.73, 63.10)
Sunshine fraction (hrs)	7.41	1.10	10.50	1.66	(7.29, 7.53)

Generally, the climate condition of the region in the fall, winter, spring, and summer seasons are the mixture of hot, cold, and moderate climates. There are also desert, humid and rainy places. As indicated in Table 1, the study region has the lowest relative humidity of 36.75 % and the highest relative humidity of 90.8 % with a mean of 61.73 to 63.10 %. The temperature (maximum) has the lowest value of 13.53 ^{0}C and the highest value of 43.13 ^{0}C with the mean from 27.23 to 28.04 ^{0}C. The rainfall amount has the minimum of 0 and the maximum of 381.4 millimeter with the mean of 62.48 to 72.37 millimeter and the magnitude of the sun fraction lasts from 1 hour and 6 minutes to 10 hours and 30 minutes with the mean of 7.29 to 7.53 hr per day. Wind speed for the year of 2000 to 2017 and across the spatial stations has a minimum of 0.1 m/s and a maximum of 7.1 m/s with the mean of 1.56 to 1.69 m/s.

Table 2. Mean Wind Speed by Month and Season.

Seasons	**Winter**			**Spring**			**Summer**				**Fall**	
Months	Dec.	Jan.	Feb.	March	April	May	June	July	Aug.	Sep.	Oct.	Nov.
Mean wind speed (m/s)	1.57	1.62	1.81	1.80	1.71	1.57	1.75	1.79	1.57	1.32	1.43	1.53
Mean wind speed per Season	**1.67**			**1.69**			**1.70**				**1.43**	

As shown in Table 2, mean wind speed in the months of February, March and July seems to have relatively higher intensity whereas months of September, October and November have relatively lower wind speed. Months of December, May and August have nearly equal wind speed distribution for the last 18 years and across the meteorological stations. From the seasons, fall has a relatively low mean wind speed whereas the remaining seasons have equal wind speed distribution which implies that wind potential is more or less stable over the three seasons of a year in Ethiopia.

Wind speed catchment spot within the potential area was identified using Horizon plots for latitude, elevation, and longitude elements. The result shows that there is more

wind speed distribution in the longitude range of 38.2 ^{0}E to 39.7 ^{0}E and in the latitude span of 7.2 ^{0}N to 8.9 ^{0}N. In addition, the wind speed is found to be high within the elevation range of 1151 to 1634 meter (Figure 2).

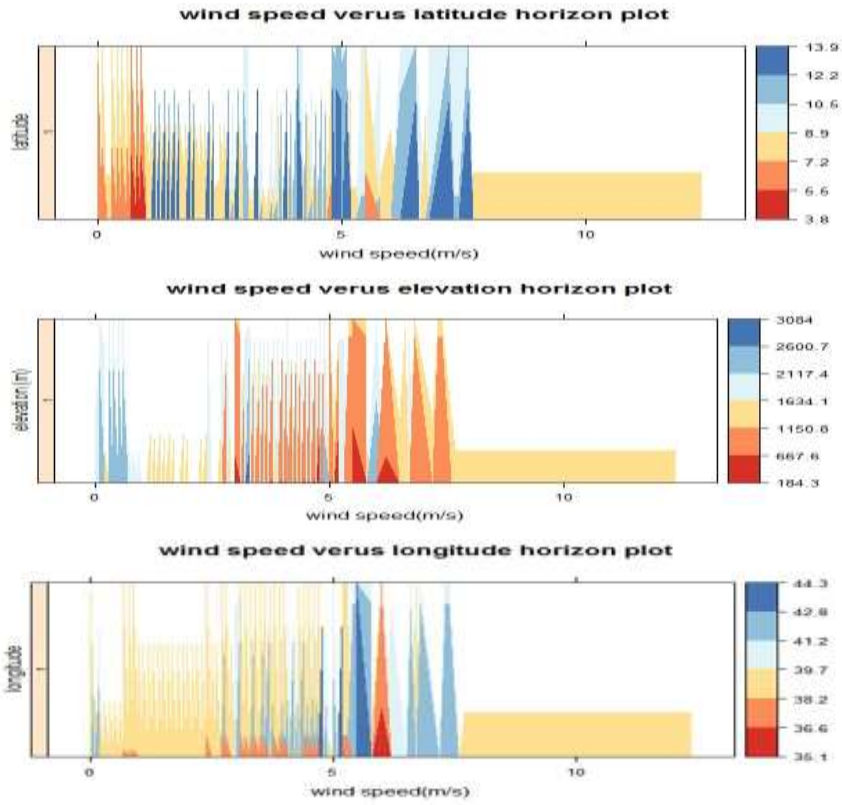

Figure 2. Horizon plots of wind speed versus topographic elements.

From wind speed map based on randomly defined intervals, it can be seen that high wind speed potential is observed at central, eastern, and northeast parts of the country. The maximum wind speed reaches up to 3.61 m/s on average. However, in the south and southeast parts, wind speed is as low as 1.22 m/s or below. As shown in Figure 3, mean wind speed magnitude is less than 5 m/s across the stations whereas more than 50% of the stations have got mean wind speed greater than 1.5 m/s and half of the stations have got mean speed in the range of 2.14 and 3.61 m/s over the years 2000 to 2017 in the study region. Particularly, the mean wind speed distribution gets higher towards the east and northeast part of the country. This result implies that regardless of the climate and topographic factors, the wind speed distribution is more or less stronger in the study region.

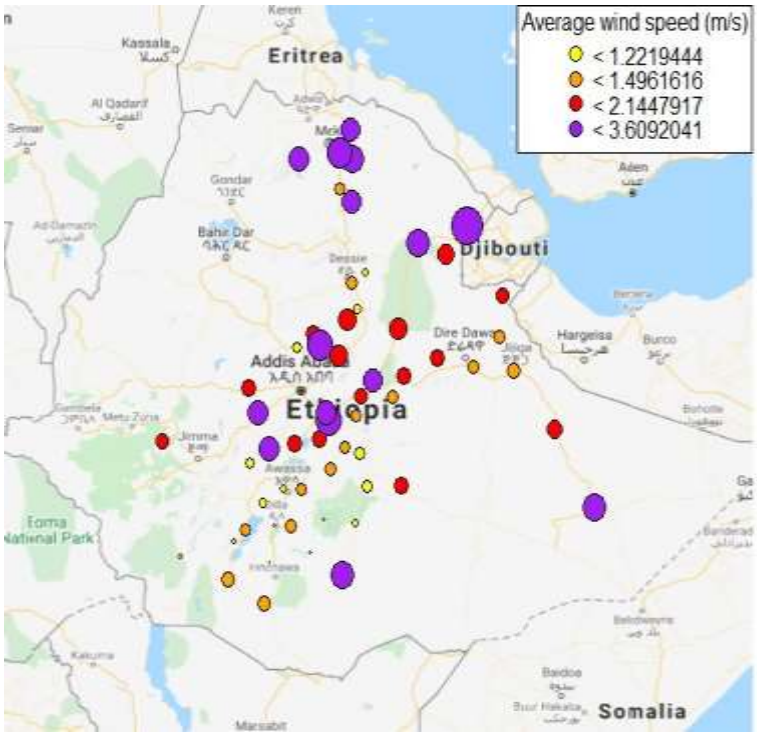

Figure 3. Spatial Plot of Mean Wind Speed Distribution in Ethiopia.

We used the Pearson's product-moment correlation of the wind speed and its spatial lag to test for the presence of spatial dependence. The result depicts that the correlation coefficient is highly significantly different from zero ($r=0.272$, $p=1.1\times10^{-15}$). This implies that there is stronger correlation of wind speed between the neighbouring stations. Furthermore, a Global Moran's I statistics is employed to test for spatial dependence after the inverse quartile spatial weight introduced in to spatial regression residual. The result shows that there is positive and statistically significant spatial autocorrelation in the residuals across the neighboring stations (Moran I statistic = 10.78, $p < 2.2\times10^{-16}$).

From both visual inspection of the plot and the tests, it is evident that spatial dependence exists in the neighbouring stations. That is, near stations have similar wind speed distribution as compared to the stations located at distant. Therefore, prediction of wind speed can be made using a stochastic spatial model by accounting for a proper measure of spatial dependence.

Maximum Likelihood Estimation

A meteorological dataset is organized into 60 stations and 12 time points to form a balanced panel data structure. Seven predictor variables are used to fit the model for wind speed variation including the time lag and spacetime simultaneous (a spatial lag in the previous period in time) components. The spatial panel data structure is partially displayed in Figure 4.

Ordering	stations	month	elevation	geogr1	geogr2	WINDLY	wspL
Abala-April	Abala	April	1441	39.76000	13.34000	1.950000	0.00
Abomsa-April	Abomsa	April	1630	39.83300	8.46670	1.385714	1.366667
Adele-April	Adele	April	2466	39.90292	7.75050	1.433333	1.566667
Aisha-April	Aisha	April	721	42.57758	10.75680	2.487500	2.050000
.							
.							
.							
Woliso-Sept	Woliso	September	2058	38.77000	13.360000	1.725000	1.776923
Worka-Sept	Worka	September	2450	39.21667	6.483333	0.400000	1.284615
Yabello-Sept	Yabello	September	1729	38.10000	4.880000	1.450000	1.438462
Ziway-Sept	Ziway	September	1640	38.70000	7.933333	1.284615	1.558333

	TMPMAX	TMPMIN	PRECIP	SUNHRS	RH	wspL1
Abala-April	32.22500	16.94000	26.16667	8.100000	70.20000	1.685030
Abomsa-April	29.77143	17.42143	76.59286	7.462500	56.88571	1.539185
Adele-April	22.92500	10.50000	76.82000	5.600000	69.40000	1.567238
Aisha-April	35.66250	21.90000	16.93750	8.075000	72.50000	1.589250
.						
.						
.						
Woliso-Sept	22.92857	12.38571	130.25714	5.528571	78.40000	1.782589
Worka-Sept	27.24000	14.27957	180.70000	9.550000	58.10000	1.632734
Yabello-Sept	26.22500	14.34444	22.76000	6.750000	71.40000	1.638119
Ziway-Sept	26.95000	14.80714	79.27692	6.600000	61.07593	1.648569

Figure 4: Spatial Panel Data Structure of Meteorological Dataset.

A dynamic spatial panel autoregressive model with random effect specification is applied for Bayesian inferences to perform the prediction of wind speed. The model estimates are presented using maximum likelihood estimation (MLE) methods in Table 3.

Table 3. Maximum Likelihood Estimates of Parameters.

Description of Parameter	Parameter	Estimate	Std. Error	t-value	Pr(>| t |)
Spatial autoregressive coefficient	λ	-0.999	0.074	10.33	8.5×10^{-05} ***
Spatial error parameter	ρ	0.761	0.345	-2.89	0.0038**
Coefficient of wind speed time-lag (m/s)	θ_1	0.279	0.033	8.43	$< 2.2\times10^{-16}$***
Coefficient of wind speed spacetime-lag (m/s)	θ_2	0.561	0.29	1.91	0.0559
Intercept	β_0	1.78	0.628	2.83	0.0047
Coefficient of elevation (m)	β_1	0.002	0.00012	1.67	0.0958
Coefficient of temperature-max (^{0}C)	β_2	0.036	0.012	3.0	0.0026**
Coefficient of precipitation (mm)	β_3	-0.002	0.0004	-4.2	2.7×10^{-05}***
Coefficient of sunshine fraction (hrs)	β_4	-0.02	0.017	-1.15	0.2496
Coefficient of relative humidity (%)	β_5	-0.003	0.00034	-0.76	0.4484

The maximum likelihood estimates are generated using *splm* function in R at 1%, 5%, and 10% levels of significance. The main focus of the study is assessing spatial autoregressive coefficients, λ and the spatial error parameter, ρ. The result reveals that both spatial autoregressive coefficients ($\hat{\lambda}$ = -0.999, t= -2.89, p=0.0038) and spatial error parameter ($\hat{\rho}$ = 0.761, t= 10.33, p= 8.5×10^{-05}) are significantly different from zero. This implies that a negative spatial dependence is inherent in the data when measuring the average influence of observations with respect to their neighbouring observations but positive autocorrelation in the spatial errors. This means, spatial lag of wind speed imposes simultaneity or endogeneity effects within spatial neighbours as well as in the spatial errors for the meteorological dataset.

The time-lag ($\hat{\varphi}_1$= 0.279, t= 8.43, p < 2.2×10^{-16}) and the spacetime-lag ($\hat{\varphi}_2$ = 0.561, t= 1.91, p=0.0559) are statistically significant at 1% and 10% levels of significance, respectively. The effects of the predictors have also been fitted so that elevation ($\hat{\beta}_1$ = 0.002, t= 1.67, p = 0.0.0958), temperature ($\hat{\beta}_2$= 0.036, t= 3.0, p =

0.0026), and precipitation ($\hat{\beta}_3$= -0.002, t= -4.2, p = 2.7×10^{-05}) found to have statistically significant effects on wind speed. However, sunshine fraction ($\hat{\beta}_4$ = -0.02, t= -1.15, p = 0.2498) and relative humidity ($\hat{\beta}_5$ = -0.003, t= -0.76, p = 0.4484) have no statistically significant effects on wind speed distribution.

For the specified spatial panel dependence model, wind distribution estimates depict that elevation and temperature have positive effects whereas precipitation, sunshine fraction, and relative humidity affect the wind speed variations negatively. That means, wind speed is more for a rise in elevation and temperature. However, more precipitation reduces the wind speed. It is also found that there is no significant influence of sunshine fraction and relative humidity on wind speed variation, which can be due to the fact that, the study region has closer values of sunshine fraction and relative humidity (Table 3).

In general, it can be concluded that the result of this study supports a previous study by Breslow & Sailor (2002) in the United States using GCM that wind power resources are vulnerable to climate change effects. The spatial and topographic variations strongly influence the wind power potential as also indicated by Yao et al. (2012). Climate covariates like precipitation (or rainfall), sunshine fraction and relative humidity generally reduces the wind speed in the long run whereas an increase in elevation and temperature increases the wind speed potential.

The study aims to base its prediction on the Bayesian estimates than the maximum likelihood estimates, since it provides an estimated parameter that converges to the truer value as the number of samples get large.

Bayesian Inference

A Kronecker product has been utilized to keep the conformity of the dimension of the inverse quartile spatial weight with the dataset to run MCMC hierarchical Bayesian estimates for the dynamic spatial panel autoregressive model. The dynamic aspect is where the spacetime recursive model in which the dependence relates to both the location itself as well as its neighbours in the previous period in time and the time-lag of the wind speed included in the model. Sampling from the joint posterior distribution of β and σ is performed using MCMC Gibbs sampler method. The algorithm is based on the decomposition of the joint posterior as the product of the conditional posterior distribution of β and marginal posterior density of σ. An *MCMCsamp* function was employed from *LearnBayes* R package to make MCMC samples of 10,000 iterations (burn-in period is 5000) from the fitted maximum likelihood estimates (Albert J., 2018). Parameter estimates of the simulated posterior draws of the spatial autoregressive, autocorrelation error parameter, and the regression coefficients of the model outputs are presented with its maximum likelihood estimates in Table 4.

Table 4. Maximum Likelihood and Bayesian Parameter Estimate.

Parameter	Maximum likelihood estimate	Bayesian estimate	Credible set at 95% conf. level
Λ	-0.999	-0.945	(-1.436, -0.362)
P	0.761	0.795	(0.655, 0.883)
θ_1	0.279	-0.006	(-0.068, 0.069)
θ_2	0.561	0.874	(0.063, 1.72)
β_0	1.78	3.1	(1.846, 4.175)
β_1	0.002	0.0001	(0.000007, 0.0002)
β_2	0.036	0.014	(0.0014, 0.0266)
β_3	-0.002	-0.0023	(-0.0031, -0.0014)
β_4	-0.02	-0.015	(-0.055, 0.022)
β_5	-0.003	-0.005	(-0.012, 0.003)
AIC	1722.1; (AIC for lm: 1756.7)	-	-

It can be seen from the result that AIC=1722.1 of the maximum likelihood estimation of the combined dynamic spatial panel autoregressive model is less than the AIC=1756.7 of the ordinary least square estimation methods which implies that the maximum likelihood method is more efficient to predict the wind speed method than the ordinary least square method. Consequently, the Bayesian estimates based on the maximum likelihood method improves the efficiency of the prediction of wind speed. The credible set of each effect from the Bayesian estimate is also given in Table 5. The interval estimates of spatial parameters λ and ρ are (-1.436, -0.362) and (0.655, 0.883) at 95% level of confidence, respectively.

Table 5. Quantiles of Parameters.

Parameter	2.5%	25%	50%	75%	97.5%
Λ	-1.436	-1.13	-0.955	-0.734	-0.362
P	0.655	0.764	0.804	0.835	0.883
β_0	1.846	2.736	3.11	3.5	4.175
θ_1	-0.0686	-0.03	-0.0063	0.013	0.069
θ_2	0.0639	0.576	0.85	1.18	1.72
β_1	0.00000072	0.0000068	0.000096	0.00012	0.00017
β_2	0.0015	0.0099	0.0143	0.018	0.0266
β_3	-0.0032	-0.0027	-0.0026	-0.0019	-0.0013
β_4	-0.055	-0.028	-0.016	-0.0017	0.022
β_5	-0.012	-0.0074	-0.0051	-0.02	0.002

Bayesian estimates indicate that the posterior medians of the estimates of the parameters are more or less similar with the mean estimates (Table 4). Besides, the traces and density plots guarantee the convergence of the estimates of the spatial parameters as well as coefficients of covariates, and the spacetime and time lags components.

The posterior (Bayesian) mean is more or less similar to the dynamic spatial panel autoregressive model of maximum likelihood estimates (Table 5). Any small differences between the posterior mean and the maximum likelihood estimates are due to small errors inherent in the simulation. The quantile values also provide the lower and upper limits of the parameter estimates at 95% level of confidence in Table 5. Therefore, the estimates are sufficient to produce predictive values of wind speed potential for some unobserved sites in the study region.

Wind Speed Prediction

To predict a wind speed for any unmeasured location, we used the measured values surrounding the prediction location estimated with appropriate model and the best measure of spatial connection. The prediction of the wind speed is performed for four distinct covariate sets. Each covariate set represents four unobserved sites (sites where we have no observations in the dataset) but found in the wind potential region. These are; Addis Ababa, Bishoftu, Harar, and Kombolcha. Addis Ababa is found at $9^0 19' N$ and $42^0 7' E$, Bishoftu at $8^0 45' N$ and $38^0 59' E$, Harar at $9^0 19' N$ and $42^0 7' E$, and Kombolcha at $11^0 5' 12'' N$ and $39^0 44' 12'' E$ coordinate points. The average values of their respective climate and spatial variables in the year of 2017 are used for the prediction. These are temperature (max), precipitation (rainfall), relative humidity, and sunshine fraction. Thus, the predicted values of wind speed at unobserved sites are presented in Table 6.

Table 6. Predicted Value of Wind Speed.

Predictors	Addis Ababa	Bishoftu	Harar	Kombolcha
Constant	3.5	3.5	3.5	3.5
Time-lag (m/s)	1.2	1	2	3.1
Spatial-time-lag (m/s)	5	2.5	3.9	4.3
Elevation (m)	2355	1920	1885	1842
Temp(max) (^{0}C)	20	24	26	19
Rainfall (mm)	57	21	44.7	29
Sunshine (hs)	60.4	54.8	52	64
Relative humidity (%)	275	302.2	304	294.5
Predicted mean of wind speed (m/s)	4.7036	4.6735	4.6816	4.4695

The results in Table 6 show that better wind resources are observed at different climate and spatial effects. Thus, it can be concluded that, according to the climate conditions of the selected sites, Addis Ababa is found to have higher mean wind speed followed by Harar whereas Kombolcha has lower wind speed measure relative to the other sites.

Therefore, using Bayesian estimates and proper selection of model reduces the statistical estimation problems and facilitates the effective assessment of wind resources which solves the problem of large uncertainty in statistical data of wind resource estimates in terms of quantity or price as indicated by Belward et al. (2011).

CONCLUSIONS AND RECOMMENDATIONS

An alternative spatial dependence measure with appropriate spatial panel model is specified to capture efficiently, the neighborhood relationship at different temporal points for the prediction of wind potential in Ethiopia. The study applied a combined dynamic spatial panel autoregressive model with inverse quartile spatial weight to predict wind speed potential spots. Climate covariates and topographic variables are used as predictors in the model fitting. The dataset was obtained from meteorological agency of Ethiopia recorded at 60 spatial points (or stations) over 18 years (2000-2007). The results depict that wind distribution is high in the beginning of summer (kiremt) season followed by spring (tsedey) season. There is also sufficient wind speed distribution during winter (bega) season. However, there is relatively mild wind distribution in the fall (belg) season. This reveals that Ethiopia is suitable for in-land wind resources for at least eight months a year. Topographically, the locations within the longitude range of 38.2 ^{0}E to 39.7 ^{0}E and latitude span of 7.2 ^{0}N to 8.9 ^{0}N are considered to be the best potential spots of wind resources alongside the Rift Valley and eastern parts of Ethiopia. The wind speed is also stronger in the elevation range of 1151 to 1634 meter. To examine the effects of spatial and spacetime interaction on wind speed distribution, it is advisable to apply a stochastic model. Thus, a combined dynamic spatial panel autoregressive model with inverse quartile separation distances spatial weight is employed to generate maximum likelihood and Bayesian estimates. The maximum likelihood estimates reveal that elevation, temperature and precipitation (or rainfall) have significant effects on wind speed distribution. Besides, Temperature induces more wind speed and a rise in elevation increases wind speed significantly. However, high precipitation reduces wind speed distribution significantly. Furthermore, Time-lag and spacetime-lag components have also highly significant effects on wind speed distribution. This implies that, there is spatial, temporal, and spacetime dependence on wind speed distribution in the study area. From the results obtained, we conclude that the effect of climate and spatial covariates on wind speed distribution is statistically significant. Thus, the potential spots of wind speed resources are highly influenced by climate and spatial predictors.

The measures of spatial dependence and spatial error autocorrelation are found to be significant different from zero. This implies that the spatial weight of inverse quartile separation distances between locations captures the spatial dependence in the neighboring stations and the error autocorrelations efficiently. Taking in to account the spatial, topographic and climate covariates in the stochastic model, the wind speed potential (variations) is recorded mainly after the rainy season ends and before it starts.

A combined dynamic spatial panel autoregressive model was applied in hierarchical Bayesian method using MCMC Gibbs sampler for 10,000 iterations as the extension of the prediction of wind speed at unobserved sites. The maximum likelihood and Bayesian estimates of the effect of the climate and spatial variables suggests a better precision of the specified model over the ordinary least square estimation method for wind speed predictions. To undertake wind resource assessment (or survey), we suggest that a combined dynamic spatial panel autoregressive model with inverse quartile separation distance efficiently captures the spatial dependence and provides a precise prediction across spatial spots and over temporal points. This approach reduces the large uncertainty in statistical data of wind resource assessment. The result also supports that spatial and temporal heterogeneity together with climate and spatial effects influence the estimates of wind resources. Finally, it is essential that the stochastic model and appropriate measure of spatial dependence based on separation distance should be applied for the assessment of highly stochastic processes like wind speed over large spatial scales. The study recommends the use of inverse quartile separation distances along with a dynamic spatial panel autoregressive model with random effects specification to refine the wind resource estimates, and to accurately locate the best harvest spatial spots and time points.

In our future works, we will explore for alternative spatial weights integrated with topographic variable (e.g. altitude differences) and continue the research of dynamic spatial weights to capture spatial dependence of larger spatial scales.

REFERENCES

1. Albert J. (2018). LearnBayes: Functions for Learning Bayesian Inference. R package version 2.15.1. https://CRAN.R-project.org/ package=LearnBayes Khandoker Shuvo Bakar, Sujit K.
2. Anselin L. and Gallo J. Le (2004). SPATIAL PANEL ECONOMETRICS. University of Illinois, Urbana-Champaign. Center for Spatially Integrated Social Science (CSISS).
3. Bekele, G., and Palm, B. (2010). Feasibility study for a standalone solarwind-based hybrid energy system for application in Ethiopia. Applied Energy, 87(2), 487495. https://doi.org/10.1016/j.apenergy.2009.06.006.
4. Bekele, G., and Tadesse, G. (2012). Feasibility study of small Hydro/PV/Wind hybrid system for off-grid rural electrification in Ethiopia. Applied Energy, 97, 515. https://doi.org/10.1016/j.apenergy.2011.11.059.
5. Belward A., Bisselink B., B´odis K., Brink A., Dallemand J., Roo A. De, Monforti E. F. (2011). Renewable energies in Africa. https://doi.org/10.2788/1881.
6. Breslow P. B., and Sailor D. J. (2002). Vulnerability of wind power resources to climate change in the continental United States. Renewable Energy, 27(4), 585–598. https://doi.org/10.1016/S0960-1481(01)00110-0.
7. Bulty B.G, Gotu B. and G. Djira (2023). A spatial autoregressive model specification with inverse quantile separation distances of locations. Spatial Statistics, 57, https://doi.org/10.1016/j.spasta.2023.100771.
8. Derbew D. (2013). Brief Facts about Ethiopia.
9. Diggle P, Paulo J., and Rebiero Jr., (2007). Model-Based Geostatistics. Springer Series in Statistics.
10. Elhorst J. P. (2011). Spatial panel models. University of Groningen, Department of Economics, Econometrics and Finance P.O. Box 800, 9700 AV Groningen, the Netherland.

Ethiopian Wind Energy Agency (2009). The Economics of Wind Energy. Annual Report.

11. Flitter H., Weckenbrock P.,Weibel R., Weismann S. et al (2016). Continues Spatial Variables. Geographic Information Technology Training alliance (GITTA) presents. http://www.gitta.info.

12. Gonza´lez-Aparicio I., Monforti F., Volker P., Zucker A., Careri F., Huld T., & Badger J. (2017). Simulating European wind power generation applying statistical downscaling to reanalysis data. Applied Energy, 199, 155–168. https://doi.org/ 10.1016/j.apenergy.2017.04.066.

13. Greasby T. A., & Sain S. R. (2011). Multivariate Spatial Analysis of Climate Change Projections. Journal of Agricultural, Biological, and Environmental Statistics, 16(4), 571–585. https://doi.org/ 10.1007/s13253-011-0072-8.

14. Jiangtao Xu Lushi, Zhao Kai, Guo Shuhua, Li Xiaojun, Wu Chengzhi and Zhang Bo (2012). Hydrochina Corporation. Master Plan Report of Wind and Solar Energy in the Federal Democratic Republic of Ethiopia.

15. Kadhem A., Abdul Wahab N.I., Aris I., Jasni J., Abdella A.(2017). Advanced Wind Speed Prediction Model Based on a Combination of Weibull Distribution and an Artificial Neural Network. Energies 2017, 10, 1744; doi:10.3390/en10111744. www.mdpi.com/journal/energies.

16. Leeds W. B., and Wikle C. K. (2012). Science-based parameterizations for dynamical spatiotemporal models. Wiley Interdisciplinary Reviews: Computational Statistics, 4(6), 554–560. https://doi.org/10.1002/wics.1227.

17. Olani A. G. (2013). State of the art on renewable and sustainable energy. Energy, 61, 2–5. https://doi.org/10.1016/j.energy.2013.10. 013.

18. Yamba F., Kamimoto M., Maurice L., Nyboer J., Urama K., Weir T., ... Kingdom U. (2011). Renewable Energy and Climate Change, 161–208.

19. Yao Y., Huang G. H., and Lin Q. (2012). Climate change impacts on Ontario wind power resource, 1–11.